PCCP

Cite this: *Phys. Chem. Chem. Phys.*, 2012, **14**, 5744–5752

www.rsc.org/pccp

PAPER

High pressure effect on phase transition behavior of lipid bilayers†

Kan Lai,[a] Biao Wang,*[a] Yong Zhang[a] and Yongwei Zhang[b]

Received 29th December 2011, Accepted 16th February 2012
DOI: 10.1039/c2cp24140d

Phase behavior of lipid bilayers at high pressure is critical to biological processes. Using coarse grained molecular dynamic simulations, we report critical characteristics of dipalmitoylphosphatidylcholine bilayers with applied high pressure, and also show their phase transition by cooling bilayer patches. Our results indicate that the phase transition temperature of dipalmitoylphosphatidylcholine bilayers obviously shifts with pressure increasing in the rate of 37 °C kbar^{-1}, which are in agreement with experimental data. Moreover, the main phase transition is revealed to be strongly dependent on lipid area. A critical lipid area of ~0.57 nm^2 is found on the main phase transition boundary. Similar structures of acyl chains lead to the same sensitivity of phase transition temperature of different lipids to the pressure. Based on the lateral density and pressure profiles, we also discuss the different effects on bilayer structure induced by high temperature and high pressure, *e.g.*, increasing temperature induces higher degree of interdigitation of lipid tails and thinner bilayers, and increasing pressure maintains the degree of interdigitation and bilayer thickness.

1 Introduction

In recent years, the interest in the effect of pressure has been largely growing in physical–chemical and biophysical studies of biological systems.[1,2] High pressure is used as a tool for understanding the spatial structures, energetics, phase behavior and dynamics of biomolecules.[3–5] In particular, high hydrostatic pressure plays an important role in deep-sea organisms living in cold and high-pressure habitats in which the pressure may be up to about 1 kbar.[6,7] Moreover, high pressure is applied in specific biotechnologies,[8,9] *e.g.*, in food processing due to its potential to inactivate microorganisms, viruses and enzymes.

In biophysics, a biomembrane seems to be one of the most pressure sensitive cellular components.[1] The basic structural element of a biological system is a lipid bilayer, which is employed as a model system of biomembranes. Amphiphilic phospholipids can self-assemble in water by the hydrophobic effect. The solutions exhibit a rich structure and phase behaviors,[10,11] depending on the hydration level, pH, ionic strength, temperature and pressure. The phase behaviors of lipid bilayers have attracted considerable interest, for the possible biological relevance of the different phases they form and the transitions they undergo.[10,12] At high temperatures, lipids form a flat fluid membrane. It is the most common phase in nature called L_α phase (liquid-crystalline phase or fluid phase), with characters of disordered chains, high occupied area per lipid and high lipid lateral mobility. It is also a common state found in most cell membranes. If the temperature decreased, one gets a phase transition (the "main" transition) from the L_α phase to a "gel" phase where the lipid molecules are more ordered, less mobile and have low occupied area. The main transition is of interest in biophysics, since the temperatures are typical on earth, and its significant influences on biological activity of cell membranes.

Numerous experimental data and theoretical models for the main transition are reported.[10,12] The physical techniques investigating on model membranes include electron spin resonance,[13] infrared,[14] Raman[15] and fluorescence spectroscopy,[16] X-ray,[17] neutron diffraction,[18] calorimetry,[19] and nuclear magnetic resonance spectroscopy.[20–22] The driving force of the main transition is known as a competition of the entropy of chains and energy of chain alignment.[23] However, the effect of one other thermodynamic and kinetic variable-pressure is somewhat less well studied.

It is known that increasing pressure shifts the chain melting transition temperatures. And interestingly, in the temperature–pressure phase diagram, a common slope of about 22 °C kbar^{-1} has been observed on the gel–fluid phase boundary of a variety of saturated and unsaturated phosphatidylcholines.[1]

Molecular simulation has been proved to be a powerful tool to provide structure and mechanism information of biological systems.[24] Phase transitions of lipid bilayers have been successfully displayed by different computational methods.[25–28] These successful models did a great support to the study of the interaction of biomembranes and biomolecules. However, less effort has been devoted to study the phase transitions of

[a] *State Key Laboratory of Optoelectronic Materials and Technologies, Sun Yat-Sen University, Guangzhou, China. E-mail: wangbiao@mail.sysu.edu.cn*
[b] *Institute of High Performance Computing, Fusionopolis, 1 Fusionopolis Way, #16-16, Connexis, Singapore*
† Electronic supplementary information (ESI) available. See DOI: 10.1039/c2cp24140d

lipid bilayers under high hydrostatic pressure. As shown recently by Rong Chen *et al*., main phase transition could be induced by hydrostatic pressure up to 1000 bar at 325 K using atomistic molecular dynamic simulation.[29] In this study we investigate the high pressure effect on the main phase transition behavior by the method of coarse grained molecular dynamics simulation.

The aim of this computational modeling study was to determine the effect of high pressure on the phase transition behavior and structural properties of bilayers. Dipalmitoylphosphatidylcholine (DPPC) is the most extensively examined phospholipid. We performed a series of coarse grained molecular dynamics simulations of a fluid phase DPPC bilayer under various high pressures. First, we calculate the phase transition temperature, isothermal compressibility, volume change, lipid occupied area and acyl chain order parameters as a function of coupling pressure. Second, we used a semi-isotropic pressure coupling method to determine the relationship between lipid occupied area and phase transition temperature. Third, we detail the influences of high temperature and pressure on bilayer structures in terms of bilayer thickness and interdigitation of lipid tails by analyzing lateral density and lateral pressure profiles, which are important to characterize the function of membrane proteins.

2 Materials and methods

We use the Martini coarse grained force field in the molecular dynamics simulation.[30,31] The Martini force field has been extensively studied and has been successfully shown to reproduce many properties of lipid membranes, including phase behavior of lipid bilayers at atmospheric pressure.[28] Fig. 1(A) shows the coarse grained representation of DPPC lipid and water.

2.1 Simulation methodology

Simulations were performed with the Gromacs simulation software,[32,33] version 4.0.3. Periodic boundary conditions were used, with constant temperature and pressure achieved by the Berendsen scheme.[34] The coupling constant is 0.1 ps for the temperature, and 0.2 ps for the pressure. The pressure coupling was applied in a semi-isotropic way to maintain zero surface tension (Fig. 1(B)). Short-range electrostatic and Lennard-Jones potentials were cut off at 1.2 nm, corresponding to the standard Martini force field. The time step of simulations was set to 40 fs.

The simulations under ambient pressure started from a fluid patch, which was obtained from a standard DPPC bilayer coordinate file from the website of Marrink's group (http://md.chem.rug.nl/~marrink/coarsegrain.html) equilibrated at 325 K during a multi-microsecond time. The equilibrated patches under ambient pressure were coupled to a higher pressure of 100, 300, 600, 1000 and 1500 bar, respectively, then equilibrated again for microseconds. Equilibrations simulated at pressure lower than 300 bar were coupled to a temperature of 325 K, and the others were coupled to a temperature of 370 K, well above the transition temperature. The final configurations after equilibration were used as the starting point of simulations under higher pressure. In order to avoid the size effect on bilayer structures, larger systems were tested. The bilayers were fully hydrated with 4000 coarse grained water beads and 256 lipids, corresponding to 62 real water molecules per lipid, resulting in 7072 beads totally. The equilibration of the bilayer system was monitored by the area per lipid. All analysis was made using the equilibrium part of the trajectories. Visual images were prepared using the VMD (Visual Molecular Dynamics) software,[35] version 1.8.7.

2.2 Calculation of lipid volumes

Lipid volumes were calculated corresponding to the description of lipid shape by Nagle and Tristram-Nagle.[10] The lipid, mixed with water in the polar and interfacial region (Fig. 1(B) and (C)), consists of two tails and a small headgroup. The system was divided into slabs perpendicular to the membrane normal, and volume was calculated in each slab. In each slab, volume of water and lipid was estimated by calculating the proportion of water beads and beads of lipid. The total volume of water and

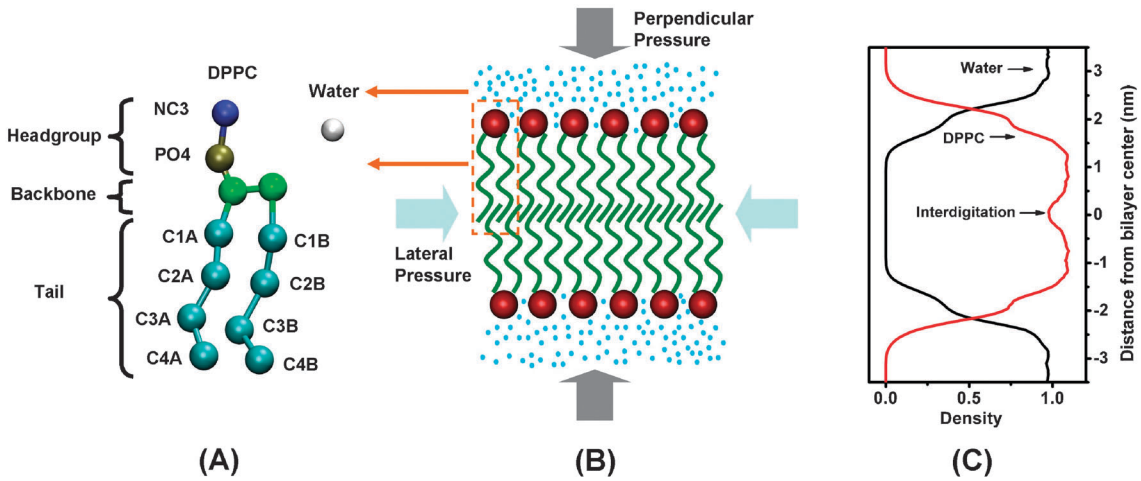

Fig. 1 (A) Coarse grained representation of DPPC lipid and water. The DPPC model consists of a hydrophilic headgroup, intermediate hydrophilic backbone, and two acyl tails model by four hydrophobic particles. (B) Schematic drawing of the lipid bilayer system. Semi-isotropic coupling pressures are shown by gray arrows (pressure in the perpendicular direction) and sky blue arrows (pressure in the lateral direction). (C) Mass density profiles of lipid (red) and water (black) across the lipid bilayer.

lipids is the sum of their volume in each slab. And the thickness of lipid was roughly calculated by dividing the lipid volume by the lipid occupied area.

2.3 Calculation of the lipid tail order parameter

The order parameter of lipid tails indicates the carbon chain orientation. The order parameter of lipid tails was calculated using the equation,

$$S_z = \tfrac{3}{2}\langle\cos^2\theta_z\rangle - \tfrac{1}{2}$$

where θ_z is defined as the angle between the z-axis of the simulation box (membrane normal) and the vector from coarse grained lipid tail beads C_{n-1} to C_{n+1} (shown in Fig. 1(A)), *e.g.* C1A–C3A. Order parameters vary between 1 and $-1/2$ indicating a fully order along the normal direction to a fully order perpendicular to the normal direction.

2.4 Calculation of lateral pressure profile

Lateral pressure profile is defined as the difference of normal P_N and lateral P_L components of pressure tensor,

$$\pi(z) = P_L(z) - P_N(z)$$

$$P_L(z) = \tfrac{1}{2}\left(P_{xx}(z) + P_{yy}(z)\right)$$

$$P_N(z) = P_{zz}(z)$$

where P_{xx} and P_{yy} are the lateral components of the pressure tensor, and P_{zz} is the normal component of the pressure tensor. A pressure field calculation code developed by Marrink's group[36] was used for the analysis of simulations. The simulation box was divided into about 200 slices with a thickness of 0.05 nm, local pressure tensor was calculated in each slice for 200 ns.

3 Results and discussion

Pressure is usually understood as an effect which occurs when a force is applied on a surface. In molecular simulation, pressure is defined as a sum of kinetic and configurational contributions. The effects of pressure are the same, when pressure applied increased, volume decreased. In this study, we addressed how pressure affected main phase transition behavior, structural and dynamical properties of a fluid-phase DPPC bilayer by systematic analysis of a series of coarse grained molecular dynamics simulations.

3.1 Phase transition temperature

In order to explore the effect of pressure on the phase transition temperature, a series of simulations were performed under a broad range of coupling pressure. Five individual simulations up to 800 ns were performed at every set of temperature and pressure in order to reduce the error induced by thermal fluctuation. Phase transition under ambient pressure was well studied by Marrink's group,[28] and we got the same result that lipid bilayers remained fluid at a temperature of $T = 300$ K, well above the estimated phase transition temperature of $T = 295$ K. When the pressure was increased to 300 bar, a transformation process from the fluid phase to the ripple gel phase was observed, indicating that a strong increase in the phase transition temperature was induced by the applied pressure.

During the phase transformation, a significant decrease of lipid occupied area was observed, the lipids froze in a few nanoseconds and packed ordered to form a major gel-like domain (see ESI†, Fig. S1 and S2). A few lipids remained in the disorder state, representing a minor fluid-like domain. The coexisting phase is very stable over time (within 10 microseconds), indicating that the system is well-equilibrated. The structure of the coexisting phase is similar to the structure found in the recent high pressure atomistic molecular dynamic simulation and experimental studies with a major gel-like region and a minor fluid-like region.[29,37–40] The results suggest that the coexisting phase is a ripple phase.

The ripple phase is an intermediate phase with periodic wavelike structure. The minimal wavelength of ripple observed in experiment is ~13 nm.[41] In our simulation study, the periodic ripple phase is found stable with a minimal wavelength of ~12 nm, consistent with the experimental data. In smaller scale systems (*e.g.* with a box dimension of 6 nm), however, the ripple phase was not observed; instead, a tilted gel phase was formed. As mentioned above, the ripple phase is a fluid–gel coexisting phase. We suggest that in the smaller gel patch, the presence of fluid patch as "defect" line would significantly increase the free energy of the bilayer system, which results from the unfavorable deformation and relative large fluid–gel phase boundary. Therefore, the fluid patch is not stable in smaller scale systems. As we use periodic boundary conditions in our simulation study, the absence of ripple phase in the smaller scale system could attribute to the unfavorable period of the simulation box. The same result was also found in the previous simulation study.[25] The results demonstrate the ability of the Martini coarse grained model to study the main phase transition from the fluid phase to the ripple phase by using a large simulation system. Accordingly, all of the results in this paper correspond to the main phase transition from the fluid phase to the ripple phase.

The results are depicted in Fig. 2. All of them correspond to the transition temperature of main transition from the fluid phase to the ripple gel phase. Fig. 2 shows that elevation of pressure caused a significant increase of the phase transition temperature. This behavior is in agreement with the experimentally observed dependence of the transition temperature

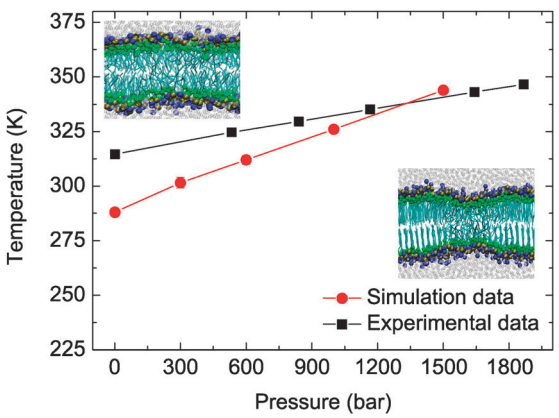

Fig. 2 Plotted are phase transition temperatures of DPPC bilayers subjected to different external pressure (red filled circles) simulations, (black filled squares) experimental data of DPPC bilayers.[42]

on the pressure. The transition temperature is rather a non-linear function of the applied pressure p, in agreement with the experimental findings.[42] The positive slope can be explained in thermodynamics using the Clausius–Clapeyron relation, $dT_m/dp = T_m\Delta V_m/\Delta H_m$, by the negative enthalpy change ΔH_m, and a volume reduction, ΔV_m, for the fluid–gel phase transition.

The transition temperature is somewhat lower than reported experimental values[42] at low coupling pressure. The estimated slope of the transition temperature dependency on pressure is $\sim$37 °C kbar^{-1}. It has been discussed that in molecular dynamics simulation, transition temperature of DPPC bilayers is a function of system size and simulation time,[28] the lower values in simulations likely originate from finite simulation time and suppression of thermal undulations by periodic boundary conditions. The temperatures of fluid–gel phase transition will rise by enlarging the system and increasing the simulation time. The disagreement will decrease by performing simulations with macroscopic system and simulation time. Moreover, as has been explored,[28] the Martini coarse grained model DPPC is unable to distinguish from model DMPC, the transition temperature for the DPPC model is between the experimental transition temperature of DMPC and DPPC, somewhat lower than that of DPPC, making the simulation value comparatively more favorable to the experimental value at low pressure.

In addition, we performed a set of simulations with different compressibility coefficient, where the compressibility setup was changed from 3×10^{-5} bar^{-1} to 7×10^{-5} bar^{-1}, a more appropriate value for the real fluid phase of DPPC. An elevation of compressibility coefficient did not virtually change the transition temperature at ambient pressure, with an increment within 1 °C. However, the transition temperature decreased significantly at high pressure, about 3 °C at 1500 bar. The result makes the dependency of transition temperature *versus* pressure comparatively more favorable to the experiment.

Additional simulations that added the ripple gel patch to high pressure above 2000 bar resulted in the freezing of the water layer, the same as decreasing temperature below 270 K at ambient pressure using the martini coarse grained model.[28] Therefore, it is unclear whether additional gel phases, *e.g.*, interdigitated phase or untilted Gel IV phase[43] under higher pressure can be observed with this model.

3.2 Isothermal compressibility and volume change

To understand the effect of pressure on the bilayer structure, volumes of lipid bilayers at same temperature and different pressures were estimated from the thermal expansion behavior under different pressures. The temperature was set to 325 K for the fluid phase and 295 K for the ripple phase. Phases which are not stable in such temperature when equilibrated (*e.g.* DPPC bilayer at 325 K and 1500 bar was in ripple phase) were considered to be the supercooled fluid phase or the superheated ripple gel phase.

The compression of lipid is reduced by increasing pressure, both in fluid and ripple phases. The isothermal compressibility is calculated using the function,

$$\kappa_T = -\frac{1}{V}\left(\frac{\partial V}{\partial p}\right)_T$$

the volume and its sensitivity to pressure of the fluid phase are higher than the corresponding value of the ripple phase. The isothermal compressibilities of the fluid phase and the ripple phase are 8.17×10^{-5} bar^{-1} and 7.43×10^{-5} bar^{-1}, respectively. The difference in isothermal compressibility 0.74×10^{-4} M Pa^{-1} is consistent with the experimental value 1.2×10^{-4} M Pa^{-1}.[42]

A drop of lipid volume was found in the fluid to ripple phase transition. The results show that the volume change is a linear function of the coupling pressure. The sensitivity of partial volume change to pressure is $-3.85(\pm0.24) \times 10^{-3}$ cm^3 mol^{-1} bar^{-1}, in agreement with experimental value -4.93×10^{-3} cm^3 mol^{-1} bar^{-1}.[42] The decrease in the volume change by increasing pressure is known as the difference in the lipid compressibility coefficient in ripple and fluid phases.

3.3 Order parameter and lateral diffusion coefficient

The order of lipid tails is a critical parameter to determine the entropy of lipids, which is known to have great influence on phase transition of lipid bilayers. The order of lipid tails increased upon increasing pressure (Fig. 3(A)), in agreement with experimental finding.[22] However, the order parameter at the phase transition point under different pressures shows that acyl chains of lipids under high pressure are less ordered than the one under ambient pressure (Fig. 3(B)).

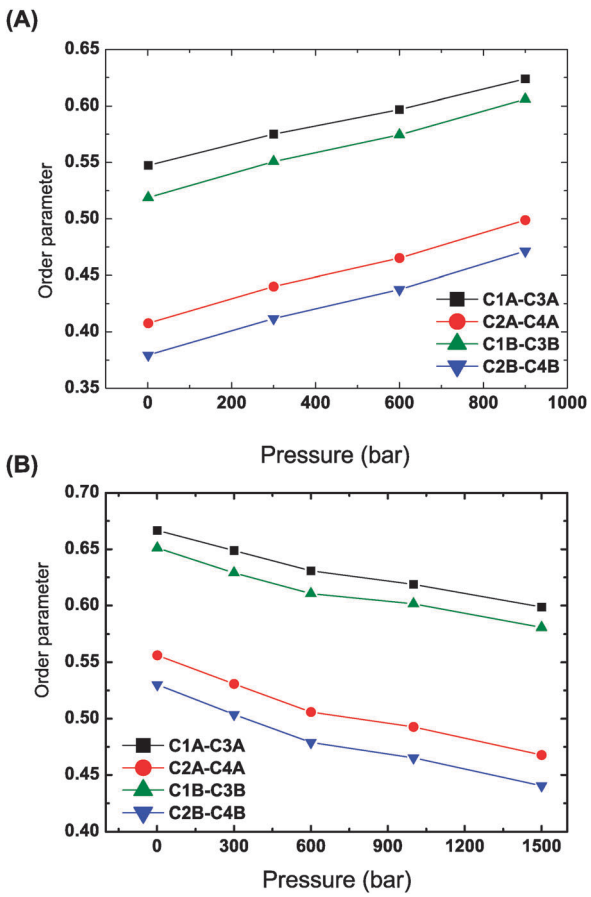

Fig. 3 Plotted are acyl chain order parameter of a liquid phase DPPC lipid bilayer at a temperature of 323 K as a function of pressure (A), acyl chain order parameter of a liquid phase DPPC lipid bilayer at the phase transition point as a function of pressure (B).

Our simulations show that lateral diffusion coefficient of liquid phase DPPC lipid decreased from 6.58(±0.80) × 10^{-7} cm^2 s^{-1} to 4.68(±1.38) × 10^{-7} cm^2 s^{-1} when the pressure is increased from 1 bar to 300 bar at 323 K. It decreases by about 29%, compared very favorable to the experiment results of 30%.[44] In the experimental studies, lipid bilayers at a temperature of 323 K and pressure beyond 300 bar would lead to the main phase transformation. A further 70% decrease in lateral diffusion coefficient of lipid occurs at this phase transition.[44] In our simulation, the lipid lateral diffusion coefficient drops from 3.01(±0.43) × 10^{-7} cm^2 s^{-1} to 0.39(±0.07) × 10^{-7} cm^2 s^{-1} during the main phase transition at a pressure of 300 bar, a ~87% decrease was observed, compared favorable with the experimental data. Lateral diffusion coefficient of lipid was found to be related to the free volume inside the bilayer[45–47] and the packing order of lipid.[48,49] Lipid occupied area decreased upon increasing pressure, indicating a decrease in the free volume inside the bilayer. Moreover, the lipid tail order parameter was found to increase under high pressure (Fig. 3(A)). We suggest that the above changes in bilayer structure result in the significant decrease of lateral diffusion coefficient of lipid.

3.4 Lipid occupied area and thickness

The surface area per lipid reproduced the experimental value of a DPPC bilayer at ambient pressure,[28] for which a value of 0.63 nm^2 at T = 325 K and 0.57 nm^2 at T = 288 K, in rough agreement with experimental value 0.64 nm^2 at T = 325 K, and 0.55 nm^2, estimated at T = 288 K.[10]

Results show that the compression effect of lipid bilayers in the fluid phase and the ripple phase is different. In the ripple phase, elevation of pressure or decreasing temperature would cause reduction of lipid occupied area and bilayer thickness.[50] However, the response to pressurization in the fluid phase is rather anisotropic. The sensitivity of lipid occupied area in the fluid phase is higher than that in the ripple phase. The thickness of a fluid phase DPPC bilayer increased significantly upon decreasing temperature, in agreement with recent experimental finding.[51] However, the bilayer thickness seems to be not affected obviously by increasing pressure. The phase transition from the fluid phase to the ripple phase was found strongly dependent on the lipid occupied area of the fluid phase. The lipid occupied areas of the fluid phase at the phase transition temperature remained constant (0.57 nm^2) as a function of pressure (Fig. 4). However, bilayer thickness is less relevant to the main phase transition.

The high isothermal compressibility of the fluid phase is likely due to the high disorder of the melting chain of the lipids thus more free volume in the bilayer. When the pressure increased, the occupied area of the bilayer surface reduced significantly, then less free volume left in the bilayer. Therefore, the melting chains pack more tightly, and lead to a slight ordering effect of the chain arrangement.

Similar results were found by applying complex pressure. Additional simulations were performed to study the relationship of phase transition and lipid occupied area. A semi-isotropic pressure coupling method was used to apply different pressures in the perpendicular direction and lateral direction. When the applied pressure in the perpendicular direction was higher, for example, 10 bar in the perpendicular direction and 1 bar in the lateral direction, a lipid bilayer was drastically spread, resulting in larger lipid occupied area, from 0.63 nm^2 to 0.65 nm^2 at T = 325 K. We observe that cooling of this patch below the phase transition temperature under ambient pressure (T_m = 288 K) does not result in ripple phase formation on a microsecond time scale. Finally, the bilayer patch transform to the ripple phase at T = 280 K. The phase transition temperature was decreased by 8 °C from 288 K at ambient pressure. However, lipid occupied area of the fluid phase at phase transition temperature was 0.57 nm^2, consistent with the former "critical" lipid occupied area found in high pressure phase transition. The pressure in the perpendicular direction leads to lower transition temperatures, by inducing the disordering effect of the lipid acyl chains, thus creating substantial free volume in the bilayer. In contrast, when the pressure applied in the perpendicular direction was lower, for example, 1 bar and 10 bar in the perpendicular direction and the lateral direction, respectively, the suppression of lipid occupied area was much stronger than that of the applied pressure when both in perpendicular and lateral directions were 10 bar. Moreover, the lipid occupied area of the fluid phase at the phase transition temperature was found consistent with the former value. Therefore, we suggest that the lipid occupied area is relevant with free energy of chain alignment. The fluid phase becomes unstable when the lipid area is under 0.57 nm^2, the over compression of lipid occupied area is likely to trigger the disorder–order phase transition of lipid bilayers.

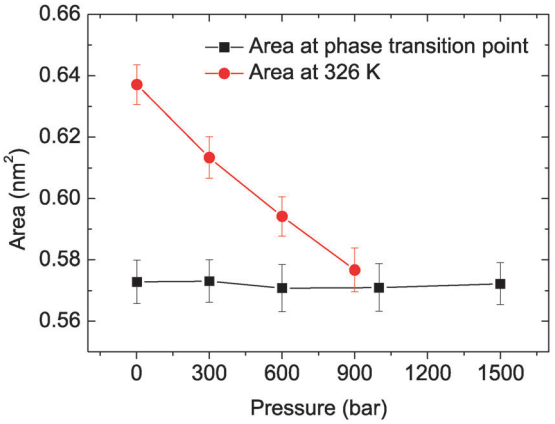

Fig. 4 Plotted are lipid areas at the phase transition point at different pressures (black filled squares). A critical lipid area of ~0.57 nm^2 was found in the main phase transition boundary. Lipid occupied area at 323 K is also plotted for comparison (red filled circles).

Previous study of external surface pressure induced phase transition of DPPC bilayers[52] showed that elevation of applied pressure in the lateral direction resulted in larger increase of phase transition temperature. A lipid bilayer is transformed from the fluid phase into the gel phase at 330 K (16 K above the experimental phase transition temperature of DPPC) under a surface pressure of 225 bar (40 mN m^{-1}), indicating a high elevation of transition temperature by lateral pressure (above 69 K $kbar^{-1}$),[52] much higher than the experimental value of isotropic high pressure induced phase transition (22 K $kbar^{-1}$)[1] and our result (39 K $kbar^{-1}$) at high pressure. It shows that the pressure applied in the perpendicular direction has the effect of suppression on the transition temperature. Our results are

consistent with the work of Risselada and co-workers[53] in their area constraint simulations using the Martini coarse grained model, in which the gel domain was found stable below a critical area around 0.57 nm^2.[53] We conclude that the area reduction is indeed the reason for the main phase transition. Thus, the main phase transition temperature *versus* pressure can be calculated by the equation,

$$\frac{dT_m}{dp} = \left(\frac{\partial T}{\partial p}\right)_A = -\left(\frac{\partial T}{\partial A}\right)_p \left(\frac{\partial A}{\partial p}\right)_T = -\frac{\left(\frac{\partial A}{\partial p}\right)_T}{\left(\frac{\partial A}{\partial T}\right)_p}$$

Elevation of phase transition temperature by high pressure can be explained by the positive isothermal compressibility and thermal expansibility of lipid area in the fluid phase.

The phase behavior of hydrated lipids depends on the lipid molecular structure.[12] It is known that phase transition temperature depends on chain length and type of headgroup. Increasing chain length leads to the increase of phase transition temperature. Moreover, introducing an unsaturated bond has the effect of lowering the chain melting transition temperature. However, the effect of pressure on the transition temperature seems not affected by the chain length and headgroup. Roland Winter shows that the sensitivities of the temperature of the chain melting transition to pressure were the same for a variety of saturated and unsaturated phosphatidylcholines.[1] One should notice that most of the lipids mentioned above are saturated diacyl PC groups with the same backbone but different chain lengths or headgroups, and others with just one *cis* or *trans* double bond in the middle of the chain. It is interesting that a common slope of about 22 °C $kbar^{-1}$ has been observed for the gel–fluid phase boundary, indicating that lipids with a saturated diacyl chain have similar lateral isothermal compression and thermal expansion characters. We suggest that the chain type is the critical factor to define the characteristics of the lateral compression of lipid bilayers.

Furthermore, introducing double bonds in a single chain or both chains will bend the chain and induce free volume, thus, significantly increase the occupied area of lipid bilayers. Therefore, more lateral compression by reducing temperature or increasing pressure will be necessary to reach the critical area of phase transition. Thus, increasing lipid chain unsaturation has the effect of lowering the chain melting transition temperature. When the double bond is located near the geometric center of the hydrocarbon chain, the lateral expansion of lipid occupied area by bending the chain has been maximized. Thus the transition temperature will be minimized, consistent with the experimental findings.[12] Therefore, the adaptation to high pressure conditions of deep sea organisms by increasing composition of unsaturated lipids can be explained by increasing lipid occupied area by imposing kinks in the linear conformations of the lipid acyl chains.

3.5 Lateral pressure profile and density profile

Furthermore, Fig. 5 shows the lateral pressure profile and density profile for a set of DPPC bilayers. At ambient pressure, the main effect of decreasing temperature is the increase of both positive and negative peaks at the membrane–water interface region in lateral pressure profiles (Fig. 5(A)). However, the peak in the middle of bilayer remains almost unchanged. A peak located in about 2.3 nm from the bilayer center, between the negative peak and positive peak in the head group region, appeared and increased up to 70 bar when the temperature decreased from 345 K to 287 K. Accordingly, we also found new peaks in the lateral density profiles located in about 2.3 nm from the bilayer center, which result from the increasing density of coarse grained beads of head groups NC3 and PO4. We suggest that the new peak in the lateral pressure profiles results from the repulsion of headgroup beads NC3 and PO4. Moreover, the distance of peaks in both sides of a bilayer increased, and the density profile also shows that density of lipid shifted and density of water reduced at the lipid/water interface (Fig. 5(B)), indicating that the thickness of a bilayer increased when the temperature decreased. The density peak in the middle of lipid bilayer also remains unchanged.

At a temperature of 323 K, when the coupling pressure increased, the perpendicular pressure profiles ($P_{zz}(z)$) raised in perfect proportion (data not shown), however, the lateral pressure profile was not affected by the coupling pressure significantly, keeping the similar change as decreasing temperature: with the peaks at the membrane–water interface region decreased and unchanged at the bilayer center (Fig. 5(C)). The influence on density profiles is rather different from that of decreasing temperature (Fig. 5(D)). The density of water at the water/lipid head interface region does not change obviously, indicating that the thickness of a bilayer remains constant. The density in the lipid tails region is increased proportional to the pressure applied.

At the phase transition point, lateral pressure profiles at different coupling pressures remain almost the same shape (Fig. 5(E)), however, with different peak–peak distances, according to different phase transition temperatures. The density profiles show that a bilayer becomes thinner at high pressure phase transition point (Fig. 5(F)), and the lipid head group does not change obviously. However, the lipid tails pack tighter according to the increase of density in the hydrophobic region.

The origin of the peak in the center of the lateral pressure profile is still not clear.[54,55] Previous studies of lateral pressure profiles suggested that the arising of the peak in the center of lipid bilayer was due to the interdigitation of lipid tails from both leaflets.[54] One should notice that the lipid occupied area is significantly increased with the increase of temperature, the density of lipid should be decreased according to the increase of the lipid occupied area. Due to the thinning and disordering effect of increasing temperature, the density of lipid decreased slightly. However, the density in the bilayer center (arrow in Fig. 5(B)) reflects that the interdigitation of lipids from both leaflets remains constant with the increasing of lipid occupied area, indicating that the degree of interdigitation increased. However, the peaks in the middle of lateral pressure profile remain constant (arrow in Fig. 5(A)).

Upon increasing coupling pressure, we find somewhat different behavior, especially in the middle of the bilayer. The difference between increasing pressure from increasing temperature is that the distance of peaks in both sides of a bilayer has not been changed (Fig. 5(C)), indicating that the bilayer thickness is not affected

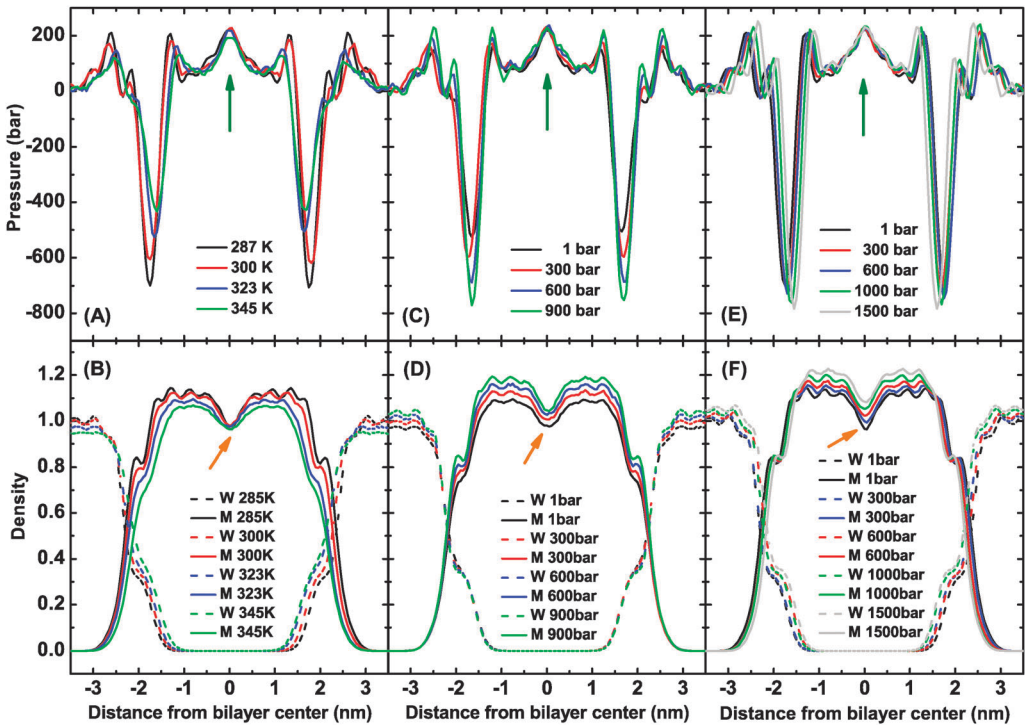

Fig. 5 (A) Lateral pressure profiles and (B) density profiles of fluid DPPC lipid bilayer (M) and water (W) as a function of temperature at ambient pressure; (C) lateral pressure profiles and (D) density profiles of fluid DPPC lipid bilayer (M) and water (W) as a function of pressure at a temperature of 323 K; (E) lateral pressure profiles and (F) density profiles of fluid DPPC lipid bilayer (M) and water (W) at the phase transition point as a function of pressure. Lateral density was normalized by the density of water in the sample at a temperature of 287 K and ambient pressure. The interdigitation of lipid tails from different monolayers depends on the density in the bilayer center and lipid area. The peak in the bilayer center in pressure profiles showed no dependency on the interdigitation of lipid tails. At the phase transition point, the interdigitation of lipid tails increases with the increasing pressure.

obviously by pressure. With the thickness unchanged, the density profiles shift according to the decrease of lipid occupied area. The order parameter of lipid tails increased (Fig. 3(A)) while the lateral pressure peak in the middle of bilayer still not changed with an increase in coupling pressure. The results show that the order parameter has no relation straightforwardly with the peak in the middle of lateral pressure profile, in agreement with the result of Ollila *et al.*[55] The density in the bilayer center is increased proportional to the applied pressure as the density in the other lipid tail region, implying that there is no change of interdigitation. Therefore, our results do not suggest any direct relation with the appearance of the peak in the membrane center and interdigitation of lipid tails. Results from lateral pressure profiles are in agreement with the previous suggestion of Ollila *et al.*[55] Their recent molecular dynamics study of polyunsaturated lipids shows that the influence of the peak in the center of lipid bilayer might not be relevant to the interdigitation.

At the phase transition point, with the lipid occupied area unchanged, lipid bilayers become thinner according to the increasing phase transition temperature. The reduction of bilayer thickness is achieved by tilting and bending in the tail region, leading to more disorder lipid tails arrangement (Fig. 3(B)) and higher density (Fig. 5(F)). Density in the middle of bilayer increased obviously, more than that for the other lipid tail region, indicating that interdigitation of lipid tails increased in the phase transition point when

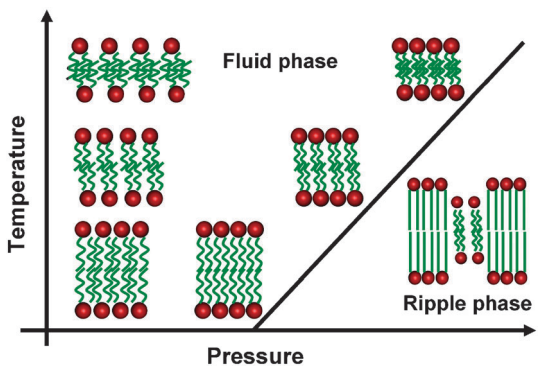

Fig. 6 Schematic show of lipid structure in the temperature–pressure phase diagram.

the coupling pressure increased. Schematic drawing of bilayer structure affected by temperature and pressure is shown in Fig. 6.

When the temperature decreased, thickness of the membrane increased significantly, which is likely to induce mismatch between the hydrophobic parts of lipid bilayer and membrane protein. The hydrophobic mismatch of membrane protein and biomembrane would cause instability of membrane protein, and could also regulate protein aggregation on biomembranes.[56–58] Bilayer thickness is also suggested to affect membrane permeability[59,60] and organization of lipid rafts.[61] In contrast, the thickness of the membrane is almost unchanged upon increasing pressure, implying that there would be less hydrophobic mismatch.

Moreover, the change of lateral pressure profile can affect membrane proteins whose function is due to a conformational change accompanied by a depth-dependent variation in the cross-sectional area of the protein.[62] The influence of lateral pressure profile by increasing pressure is less obvious than by increasing temperature, suggesting that high pressure has less perturbation on biomembranes.

Furthermore, the increasing effect on lipid tail interdigitation by higher temperature and decreasing effect on bilayer thickness by higher pressure found in these simulations likely lead to the additional interdigitated gel phase transition under high pressure and high temperature conditions.[1]

4 Conclusions

We have performed molecular dynamics simulations using a coarse grained model for the high pressure effect on the structure and phase transition behavior of a DPPC lipid bilayer. According to our simulations, important physical quantities, *e.g.*, phase transition temperature, volume changes, lateral diffusion coefficient and lipid tail order parameter are calculated as functions of the coupling pressure. The results show that main phase transition temperature of DPPC increased with increasing pressure. The pressure induced phase transition is found to depend on the lipid area based on the semi-isotropic pressure coupling method. A critical lipid area in the fluid phase of $\sim$0.57 nm^2 is found on the high pressure main phase transition boundary of DPPC. We suggest that the same dependency of phase transition temperature on pressure of different lipids is due to the similar type of acyl chain, for the similar lateral compression character. By analyzing the density and lateral pressure profiles, we found that high pressure induced less change than high temperature did in the bilayer thickness, degree of acyl chain interdigitation and lateral pressure, which implied that high pressure has less influence on the membrane protein whose function depends on the hydrophobic mismatch and lateral pressure. Moreover, no clear relation was found between acyl chain interdigitation and the pressure peak in the bilayer center. These results show that the effect of increasing pressure on main phase transition cannot be mimicked simply by decreasing temperature. The differences between the effect of pressure and that of temperature on the bilayer structure may be a leading role of additional high pressure phase transition to a interdigitated gel phase under high temperature and high pressure conditions. Our results demonstrate that molecular dynamic simulation at high pressure is a promising tool to study the phase transition behavior and structure of model biomembrane systems.

Acknowledgements

We thank Guangyuan He, Han Shen, Shaopeng Lin, Xin Luo, Xiaoyue Zhang for helpful suggestions. Financial support from the National Natural Science Foundation of China (10972239, 10732100, 11072271) is gratefully acknowledged.

References

1 R. Winter and C. Jeworrek, *Soft Matter*, 2009, **5**, 3157–3173.
2 K. Heremans and L. Smeller, *Biochim. Biophys. Acta, Protein Struct. Mol. Enzymol.*, 1998, **1386**, 353–370.
3 H. Frauenfelder, N. A. Alberding, A. Ansari, D. Braunstein, B. R. Cowen, M. K. Hong, I. E. T. Iben, J. B. Johnson and S. Luck, *J. Phys. Chem.*, 1990, **94**, 1024–1037.
4 V. V. Mozhaev, K. Heremans, J. Frank, P. Masson and C. Balny, *Proteins: Struct., Funct., Genet.*, 1996, **24**, 81–91.
5 P. T. C. So, S. M. Gruner and S. Erramilli, *Phys. Rev. Lett.*, 1993, **70**, 3455–3458.
6 A. R. Cossins and A. G. Macdonald, *J. Bioenerg. Biomembr.*, 1989, **21**, 115–135.
7 G. N. Somero, *Annu. Rev. Physiol.*, 1992, **54**, 557–577.
8 D. Knorr, V. Heinz and R. Buckow, *Biochim. Biophys. Acta, Proteins Proteomics*, 2006, **1764**, 619–631.
9 J. C. Cheftel and J. Culioli, *Meat Sci.*, 1997, **46**, 211–236.
10 J. F. Nagle and S. Tristram-Nagle, *Biochim. Biophys. Acta, Rev. Biomembr.*, 2000, **1469**, 159–195.
11 R. Koynova and M. Caffrey, *Chem. Phys. Lipids*, 1994, **69**, 1–34.
12 R. Koynova and M. Caffrey, *Biochim. Biophys. Acta,– Rev. Biomembr.*, 1998, **1376**, 91–145.
13 J. R. Trudell, D. G. Payan, J. H. Chin and E. N. Cohen, *Biochim. Biophys. Acta, –Biomembr.*, 1974, **373**, 436–443.
14 D. Siminovitch, P. Wong and H. Mantsch, *Biochim. Biophys. Acta,– Biomembr.*, 1987, **900**, 163–167.
15 P. Yager and W. Peticolas, *Biophys. J.*, 1980, **31**, 359–370.
16 J. R. Lakowicz and R. B. Thompson, *Biochim. Biophys. Acta,– Biomembr.*, 1983, **732**, 359–371.
17 J. Stamatoff, D. Guillon, L. Powers, P. Cladis and D. Aadsen, *Biochem. Biophys. Res. Commun.*, 1978, **85**, 724–728.
18 L. F. Braganza and D. L. Worcester, *Biochemistry*, 1986, **25**, 2591–2596.
19 D. B. Mountcastle, R. L. Biltonen and M. J. Halsey, *Proc. Natl. Acad. Sci. U. S. A.*, 1978, **75**, 4906–4910.
20 J. Jonas, C. L. Xie, A. Jonas, P. J. Grandinetti, D. Campbell and D. Driscoll, *Proc. Natl. Acad. Sci. U. S. A.*, 1988, **85**, 4115–4117.
21 D. A. Driscoll, J. Jonas and A. Jonas, *Chem. Phys. Lipids*, 1991, **58**, 97–104.
22 X. Peng, A. Jonas and J. Jonas, *Biophys. J.*, 1995, **68**, 1137–1144.
23 J. F. Nagle, *Annu. Rev. Phys. Chem.*, 1980, **31**, 157–196.
24 S. J. Marrink, A. H. de Vries and D. P. Tieleman, *Biochim. Biophys. Acta,– Biomembr.*, 2009, **1788**, 149–168.
25 O. Lenz and F. Schmid, *Phys. Rev. Lett.*, 2007, **98**, 058104.
26 A. H. de Vries, S. Yefimov, A. E. Mark and S. J. Marrink, *Proc. Natl. Acad. Sci. U. S. A.*, 2005, **102**, 5392–5396.
27 M. Kranenburg, C. Laforge and B. Smit, *Phys. Chem. Chem. Phys.*, 2004, **6**, 4531–4534.
28 S. J. Marrink, J. Risselada and A. E. Mark, *Chem. Phys. Lipids*, 2005, **135**, 223–244.
29 R. Chen, D. Poger and A. E. Mark, *J. Phys. Chem. B*, 2011, **115**, 1038–1044.
30 S. J. Marrink, H. J. Risselada, S. Yefimov, D. P. Tieleman and A. H. de Vries, *J. Phys. Chem. B*, 2007, **111**, 7812–7824.
31 S. J. Marrink, A. H. de Vries and A. E. Mark, *J. Phys. Chem. B*, 2004, **108**, 750–760.
32 H. J. C. Berendsen, D. van der Spoel and R. van Drunen, *Comput. Phys. Commun.*, 1995, **91**, 43–56.
33 E. Lindahl, B. Hess and D. van der Spoel, *J. Mol. Model.*, 2001, **7**, 306–317.
34 H. J. C. Berendsen, J. P. M. Postma, W. F. van Gunsteren, A. DiNola and J. R. Haak, *J. Chem. Phys.*, 1984, **81**, 3684–3690.
35 W. Humphrey, A. Dalke and K. Schulten, *J. Mol. Graphics*, 1996, **14**, 33–38.
36 O. H. S. Ollila, H. J. Risselada, M. Louhivuori, E. Lindahl, I. Vattulainen and S. J. Marrink, *Phys. Rev. Lett.*, 2009, **102**, 078101.
37 M. Schneider, W. Chan and W. Webb, *Biophys. J.*, 1983, **43**, 157–165.
38 C. Leidy, T. Kaasgaard, J. H. Crowe, O. G. Mouritsen and K. Jrgensen, *Biophys. J.*, 2002, **83**, 2625–2633.
39 M. Rappolt, G. Pabst, G. Rapp, M. Kriechbaum, H. Amenitsch, C. Krenn, S. Bernstorff and P. Laggner, *Eur. Biophys. J.*, 2000, **29**, 125–133.
40 W. J. Sun, S. Tristram-Nagle, R. M. Suter and J. F. Nagle, *Proc. Natl. Acad. Sci. U. S. A.*, 1996, **93**, 7008–7012.
41 J. Katsaras, S. Tristram-Nagle, Y. Liu, R. L. Headrick, E. Fontes, P. C. Mason and J. F. Nagle, *Phys. Rev. E: Stat. Phys., Plasmas, Fluids, Relat. Interdiscip. Top.*, 2000, **61**, 5668–5677.
42 S. Potekhin, A. Senin, N. Abdurakhmanov and R. Khusainova, *Biochim. Biophys. Acta,– Biomembr.*, 2008, **1778**, 2588–2593.

43 C. Czeslik, O. Reis, R. Winter and G. Rapp, *Chem. Phys. Lipids*, 1998, **91**, 135–144.
44 J. Jonas, *High Pressure NMR*, Springer-Verlag, Berlin, 1991.
45 H. J. Galla, W. Hartmann, U. Theilen and E. Sackmann, *J. Membr. Biol.*, 1979, **48**, 215–236.
46 P. F. F. Almeida, W. L. C. Vaz and T. E. Thompson, *Biochemistry*, 1992, **31**, 6739–6747.
47 H. S. Muddana, R. R. Gullapalli, E. Manias and P. J. Butler, *Phys. Chem. Chem. Phys.*, 2011, **13**, 1368–1378.
48 A. Filippov, G. Oradd and G. Lindblom, *Langmuir*, 2003, **19**, 6397–6400.
49 E. Falck, M. Patra, M. Karttunen, M. T. Hyvnen and I. Vattulainen, *Biophys. J.*, 2004, **87**, 1076–1091.
50 W. Sun, S. Tristram-Nagle, R. Suter and J. Nagle, *Biophys. J.*, 1996, **71**, 885–891.
51 J. Pan, S. Tristram-Nagle, N. Kucerka and J. F. Nagle, *Biophys. J.*, 2008, **94**, 117–124.
52 J. J. L. Cascales, T. F. Otero, A. J. F. Romero and L. Camacho, *Langmuir*, 2006, **22**, 5818–5824.
53 H. J. Risselada and S. J. Marrink, *Soft Matter*, 2009, **5**, 4531–4541.
54 E. van den Brink-van der Laan, J. A. Killian and B. de Kruijff, *Biochim. Biophys. Acta,– Biomembr.*, 2004, **1666**, 275–288.
55 S. Ollila, M. T. Hyvonen and I. Vattulainen, *J. Phys. Chem. B*, 2007, **111**, 3139–3150.
56 M. R. R. de Planque and J. A. Killian, *Mol. Membr. Biol.*, 2003, **20**, 271–284.
57 T. K. M. Nyholm, S. Ozdirekcan and J. A. Killian, *Biochemistry*, 2007, **46**, 1457–1465.
58 L. V. Schafer, D. H. de Jong, A. Holt, A. J. Rzepiela, A. H. de Vries, B. Poolman, J. A. Killian and S. J. Marrink, *Proc. Natl. Acad. Sci. U. S. A.*, 2011, **108**, 1343–1348.
59 K. Olbrich, W. Rawicz, D. Needham and E. Evans, *Biophys. J.*, 2000, **79**, 321–327.
60 W. Rawicz, B. Smith, T. McIntosh, S. Simon and E. Evans, *Biophys. J.*, 2008, **94**, 4725–4736.
61 A. J. Garcła-Sez, S. Chiantia and P. Schwille, *J. Biol. Chem.*, 2007, **282**, 33537–33544.
62 R. S. Cantor, *J. Phys. Chem. B*, 1997, **101**, 1723–1725.

